View metadata, citation and similar papers at core.ac.uk

brought to you by CORE

provided by Purdue E-Pubs

Purdue University
Purdue e-Pubs

Department of Electrical and Computer Engineering Faculty Publications

Department of Electrical and Computer Engineering

1992

A study of minority carrier lifetime versus doping concentration in n-type GaAs grown by metalorganic chemical vapor deposition

Gregory Benedict Lush
Purdue University

H. F. MacMillan
Varian Research Center, Palo Alto, CA

B. M. Keyes
National Renewable Energy Laboratory, Golden, CO

D. H. Levi
National Renewable Energy Laboratory, Golden CO

Michael R. Melloch
Purdue University, melloch@purdue.edu

See next page for additional authors

Follow this and additional works at: https://docs.lib.purdue.edu/ecepubs

Part of the Electrical and Computer Engineering Commons

Lush, Gregory Benedict; MacMillan, H. F.; Keyes, B. M.; Levi, D. H.; Melloch, Michael R.; Ahrenkiel, R. K.; and Lundstrom, Mark S., "A study of minority carrier lifetime versus doping concentration in n-type GaAs grown by metalorganic chemical vapor deposition" (1992). *Department of Electrical and Computer Engineering Faculty Publications.* Paper 92.
http://dx.doi.org/10.1063/1.351704

This document has been made available through Purdue e-Pubs, a service of the Purdue University Libraries. Please contact epubs@purdue.edu for additional information.

Authors
Gregory Benedict Lush, H. F. MacMillan, B. M. Keyes, D. H. Levi, Michael R. Melloch, R. K. Ahrenkiel, and Mark S. Lundstrom

This article is available at Purdue e-Pubs: https://docs.lib.purdue.edu/ecepubs/92

A study of minority carrier lifetime versus doping concentration in n-type GaAs grown by metalorganic chemical vapor deposition

G. B. LushH. F. MacMillanB. M. Keyes and D. H. LeviM. R. MellochR. K. AhrenkielM. S. Lundstrom

Citation: **72**, (1992); doi: 10.1063/1.351704
View online: http://dx.doi.org/10.1063/1.351704
View Table of Contents: http://aip.scitation.org/toc/jap/72/4
Published by the American Institute of Physics

RIGHTSLINK
Copyright Clearance Center

A study of minority carrier lifetime versus doping concentration in n-type GaAs grown by metalorganic chemical vapor deposition

G. B. Lush
School of Electrical Engineering, Purdue University, West Lafayette, Indiana 47901

H. F. MacMillan
Varian Research Center, Palo Alto, California 94303

B. M. Keyes and D. H. Levi
National Renewable Energy Laboratory, Golden, Colorado 80401

M. R. Melloch
School of Electrical Engineering, Purdue University, West Lafayette, Indiana 47901

R. K. Ahrenkiel
National Renewable Energy Laboratory, Golden, Colorado 80401

M. S. Lundstrom
School of Electrical Engineering, Purdue University, West Lafayette, Indiana 47901

(Received 15 July 1991; accepted for publication 27 April 1992)

Time-resolved photoluminescence decay measurements are used to explore minority carrier recombination in n-type GaAs grown by metalorganic chemical vapor deposition, and doped with selenium to produce electron concentrations from 1.3×10^{17} cm^{-3} to 3.8×10^{18} cm^{-3}. For electron densities $n_0<10^{18}$ cm^{-3}, the lifetime is found to be controlled by radiative recombination and photon recycling with no evidence of Shockley–Read–Hall recombination. For higher electron densities, samples show evidence of Shockley–Read–Hall recombination as reflected in the intensity dependence of the photoluminescence decay. Still, we find that radiative recombination and photon recycling are important for all electron concentrations studied, and no evidence for Auger recombination was observed.

I. INTRODUCTION

An understanding of how the minority carrier lifetime varies with electron concentration is essential for designing bipolar devices such as solar cells, transistors, and lasers. In particular, it is important to understand how the radiative, Shockley–Read–Hall (SRH), and Auger lifetimes vary with electron concentration. For p-type GaAs grown by liquid phase epitaxy (LPE),[1,2] extensive and consistent data show that p-type films are typically dominated by radiative recombination for hole concentrations over the range $10^{15}\leqslant p_0\leqslant10^{19}$ cm^{-3}. For hole lifetimes in n-type GaAs, however, the corresponding data are scarce and inconclusive. Figure 1 summarizes Hwang's measurements of minority hole lifetimes in Te-doped, melt-grown GaAs,[3–5] Casey's measurements for n-GaAs grown by LPE,[6] and Puhlmann's study of Sn-doped, LPE GaAs.[7] Also shown are recent data by Ahrenkiel *et al.* for n-GaAs with electron concentration of $n_0=2.0\times10^{17}$ cm^{-3}, grown by metalorganic chemical vapor deposition (MOCVD).[8] In contrast to the data for p-type GaAs, the authors of the studies reviewed in Fig. 1 found that n-GaAs was controlled by SRH recombination. Comprehensive data for MOCVD films are not available.

Because the available data for n-GaAs are strongly influenced by SRH recombination, intrinsic processes such as radiative and Auger recombination are difficult to study. For instance, both Garbuzov[9] and Hwang[5] deduced the radiative lifetimes in their samples, but their estimates differ by more than one order of magnitude. Also, theoretical estimates of the Auger coefficients vary widely,[10–12] and little data are available to test these estimates.[7,9,13] Neither Hwang nor Garbuzov found evidence of Auger recombination in n-type GaAs, but Puhlmann deduced an unexpectedly high Auger coefficient. It seems clear that our understanding of intrinsic recombination processes in n-type GaAs is unsatisfactory. Comprehensive studies using high-quality epitaxial material grown by modern epitaxial techniques should permit us to study intrinsic recombination processes without being dominated by defect-related, SRH recombination.

In this article we report on the first phase of a comprehensive study of the concentration-dependent minority carrier lifetime in n-type AlGaAs/GaAs/AlGaAs double heterostructures (DHs) grown by MOCVD. The selenium-doped films were n type with carrier concentrations from 1.3×10^{17} cm^{-3}. For each electron density, films with five different active layer thicknesses were grown. Unlike the earlier work cited above, we find no evidence for SRH recombination for $n_0<10^{18}$ cm^{-3}. For $n_0>10^{18}$ cm^{-3}, we do see evidence of SRH recombination, but even for the most heavily doped films, radiative recombination is important. These comprehensive results for 30 different films with various electron densities and thicknesses provide data that are directly useful for device design, and they are the first step in developing a detailed understanding of minority carrier recombination in n-type GaAs.

The article is organized as follows. Section II discusses the procedures used to analyze the photoluminescence

 0021-8979/92/161436-07$04.00 © 1992 American Institute of Physics

RIGHTSLINK

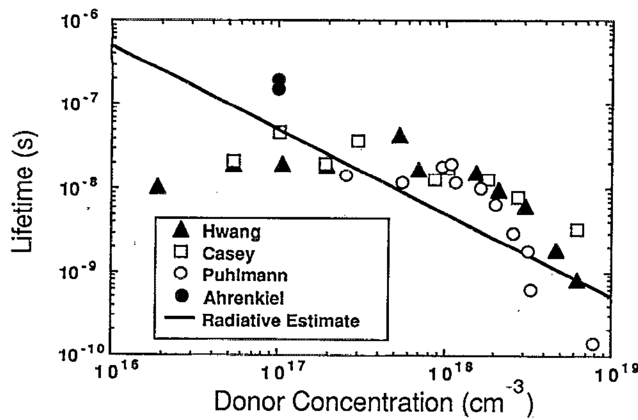

FIG. 1. Summary of previous measurements of the low-injection, minority hole lifetime in n-type GaAs grown by liquid phase epitaxy. The results of Hwang (Ref. 4), Casey (Ref. 6), Puhlmann (Ref. 7), and Ahrenkiel (Ref. 8) are displayed.

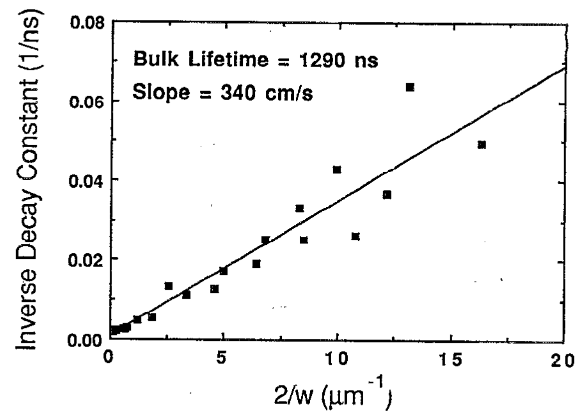

FIG. 2. Inverse photoluminescence decay rate, $1/\tau_{DH}$ vs $2/w$ for the p-type data with $p_0=5.0\times10^{15}$ cm^{-3} reported by Nelson (Ref. 17).

(PL) decay characteristics of the DHs. MOCVD growth techniques are described in Sec. III, and the specific DHs grown for the study are shown. The experimental apparatus and techniques for measuring the time-resolved photoluminescence decay are also described in Sec. III. In Sec. IV we present the measured results for both low- and high-intensity laser excitation. Evidence for photon recycling in these films is discussed in Sec. IV, and further evidence is given in Sec. V. Finally, we summarize the results and conclusions and identify issues for future research in Sec. VI.

II. PROCEDURE FOR DOUBLE HETEROSTRUCTURE ANALYSIS

Observing the time-resolved PL decay of double heterostructures (DHs) is a well-developed technique for examining interface and bulk recombination.[8,14,15] The DH is especially valuable as a tool for characterizing material quality because its PL decay can be made to be independent of diffusion. If $0<Sw/D<1$, one can express the low-injection decay constant of a DH as[16–18]

$$\frac{1}{\tau_{DH}}=\frac{1}{\tau_{bulk}}+\frac{2S}{w}, \tag{1}$$

where S is the average of the front and back interface recombination velocities, w is the active layer thickness for the DH, D is the minority carrier diffusivity, and τ_{bulk} is made up of contributions from the radiative, SRH, and Auger mechanisms. Equation (1) clearly shows contributions to τ_{DH} from both the interfaces and from the combination of the various bulk mechanisms.

To separate interface and bulk recombination, the decay constants of several DHs with identical electron densities but varying thicknesses are measured, and a plot of $1/\tau_{DH}$ vs $2/w$ is constructed.[14,19] According to Eq. (1), the intercept of this line is $1/\tau_{bulk}$ and the slope is the average of S_f and S_b, the front and back interface recombination velocities, respectively. Such a plot, using the data reported by Nelson[17] for p-type GaAs with a hole concentration of $p_0 = 5.0\times10^{15}$ cm^{-3}, is shown in Fig. 2. Despite the scatter in their data, one can clearly deduce a slope and an intercept. The data we present show much less scatter, and, interestingly, we find that all plots of $1/\tau_{DH}$ vs $2/w$ are decidedly nonlinear. For such data, it is not immediately clear how to deduce the bulk lifetime or the interface recombination velocity.

The nonlinearity of $1/\tau_{DH}$ vs $2/w$ implies that either S or τ_{bulk} depends on the active layer thickness of the DH. However, the values of S we deduced for our samples are too small to account for the changes observed in τ_{DH} vs DH thickness. Wolford *et al.* also observed nonlinearity in their plots of $1/\tau_{DH}$ vs $1/w$, but they attributed it to a change in the bulk lifetime due to modulation doping in their *P-n-P* double heterojunctions with thin n-active layers.[14] Since our samples are isotype *N-n-N* DHs, this explanation does not apply.

A thickness-dependent bulk lifetime caused by photon recycling could also explain the nonlinear $1/\tau_{DH}$ vs $2/w$ characteristic. Photon recycling, the reabsorption of photons emitted during radiative recombination events, increases the observed minority carrier lifetime when radiative recombination is important.[8,20–22] When including photon recycling, the bulk lifetime is expressed as

$$\frac{1}{\tau_{bulk}}=\frac{1}{\phi_r\tau_r}+\frac{1}{\tau_{SRH}}+\frac{1}{\tau_{Auger}}, \tag{2}$$

where ϕ_r, Asbeck's recycling cofactor, is the inverse of the probability that an isotropically emitted photon escapes from the active layer of the DH,[20] and the lifetimes have their usual meanings. DHs with thick active layers will exhibit longer lifetimes because the emitted photons are more likely to be reabsorbed before escaping through the interfaces. Because τ_{bulk} increases with w, the plot of $1/\tau_{DH}$ vs $2/w$ is nonlinear, so τ_{bulk} and S cannot be determined from its slope and intercept. An upper limit for S can, however, be estimated from the slope at large $2/w$, and, as explained in Sec. IV, the importance of nonradiative recombination can be gauged from a plot of τ_{DH} vs w, and from the intensity dependence of the decay constant.

RIGHTSLINK

n-$Al_{0.3}Ga_{0.7}As$	2×10^{18} cm^{-3}	500 Å
n-GaAs Active Layer		
n-$Al_{0.3}Ga_{0.7}As$	2×10^{18} cm^{-3}	1500 Å
n-$Al_{0.85}Ga_{0.15}As$	2×10^{18} cm^{-3}	500 Å
p^+ GaAs Buffer Layer		
p^+ GaAs Substrate		

FIG. 3. The structure of the double heterostructure samples used for the photoluminescence decay studies.

III. FILM GROWTH METHODS AND MEASUREMENT TECHNIQUES

The double heterostructures for these studies were grown at 740 °C under atmospheric pressure by MOCVD in a horizontal reactor at the Varian Research Center. The material quality produced by this reactor has been consistently high, as evidenced by production of record efficiency solar cells.[23] Film growth took place on zinc-doped, horizontal-Bridgman substrates, which were heated by radio frequency induction. The susceptor was molybdenum, coated with GaAs. The growth rate was maintained at 6 μm per hour, except for the films with $n_0 = 2.4\times10^{18}$ cm^{-3}, for which the growth rate was 4 μm per hour. The doping agent was hydrogen selenide (from Scott Specialty Gases) diluted to 55 ppm with hydrogen, and the sources were trimethyl aluminum, trimethyl gallium, and 100% arsine. The V/III ratio was maintained at 30, with the exception of the films with $n_0 = 2.4\times10^{18}$ cm^{-3}, for which the V/III ratio was 45. Hydrogen was purified by diffusion through palladium to provide a background flow rate of 12 ℓ/min.

The basic structure of the DHs is shown in Fig. 3, and Table I lists the specific DHs grown for this study. All electron concentrations were measured by the van der Pauw technique. $Al_{0.3}Ga_{0.7}As$ layers provide passivation and carrier confinement. The back two AlGaAs layers serve these purposes and serve as etch stop or etch release layers as well.[24,25] (All results presented in this article are for DHs attached to the GaAs substrate, but the etch stop/release layers will permit future studies of thin-film DHs that are separated from the substrate.)

TABLE I. Targeted thicknesses and measured electron densities for each of the 30 double heterostructures used for this study.

n_0 (cm^{-3})	Targeted thicknesses (μm)				
1.3×10^{17}	0.25	1.25	2.5	5.0	10
3.7×10^{17}	0.25	1.25	2.5	5.0	10
1.0×10^{18}	0.5	1.0	2.0	4.0	8
2.2×10^{18}	0.25	1.25	2.5	5.0	10
2.4×10^{18}	0.25	0.5	1.25	2.5	10
3.8×10^{18}	0.25	0.5	1.25	2.5	10

Photoluminescence decay was observed by the time-correlated, single photon counting technique described previously.[26,27] The exciting source was a Spectra Physics 375B cavity-dumped dye laser pumped by a frequency-doubled, Spectra Physics 3400 Nd^{3+}:YAG laser. Using Rhodamine 6G dye, pulses with a 10 ps full width at half maximum (FWHM) tuned to 600 nm wavelength were produced. The diameter of the unfocused beam was $\simeq$0.75 cm, and when focused, the beam diameter was $\simeq$0.05 cm. The laser repetition rate was 800 kHz. To examine intensity-dependent effects, a continuous gradient neutral density filter was used to vary the average laser power from a maximum of 40 mW to less than 0.1 mW. The corresponding energy per pulse varied from 50 to 0.1 nJ, respectively.

The emitted luminescence was collected in a back-scattering geometry and focused on the slits of a 0.22 m scanning double monochrometer tuned to 870 nm, the peak of GaAs band edge emission. The resolution of the monochromator was 3.6 nm/mm, and the slit width was varied from 50 to 400 μm, according to the intensity of the luminescence observed. Single-photon detection is by an S1 photomultiplier tube with a 300 ps transit-time dispersion. The single-photon induced voltage pulses are amplified and fed to a multichannel pulse height analyzer.

For an active layer thickness of 10 μm, an excitation wavelength of 600 nm, and a repetition rate of 800 kHz, the average injected electron-hole concentration is $\simeq 6\times10^{14}$ cm^{-3} when using a 20 mW, average power, unfocused beam. When the beam is focused to 0.05 cm, the average injected carrier concentration increases to over 10^{17} cm^{-3}. For a 1-μm-thick active layer, the 20 mW focused beam produces an average injected carrier density of greater than 10^{18} cm^{-3}. For thin samples, some of the incident light is not absorbed in the DH, so to estimate the injection level we make use of published data for the absorption coefficient.[28]

IV. RESULTS

Table II lists the low intensity decay constants and their uncertainties for each of the films examined. Uncertainty in the decay constant is a result of noise in the PL decay data or, in a few cases, occurs because the PL decay was slightly nonexponential. Also listed is the expected low injection radiative lifetime at each electron concentration, obtained from[21]

$$\tau_r = 1/Bn_0, \quad (3)$$

where $B = 2.0\times10^{-10}$ cm^3/s. All films show a decay constant above the radiative estimate and for the thickest films, τ_{DH} is as much as twelve times the radiative lifetime expected theoretically.

Figure 4 shows plots of $1/\tau_{DH}$ vs $2/w$ for each of the six electron densities investigated. When compared to the

RIGHTSLINK

TABLE II. Measured room temperature decay constants and their uncertainties for each of the DH samples. In each case, the values reported are those at low laser intensity. The targeted thicknesses are given in brackets for clarity. Shown in the last column are the lifetimes expected theoretically by Eq. (3).

n_0 (cm^{-3})	[Targeted DH thicknesses (μm)] Measured DH decay constants (ns)					$1/Bn_0$ (ns)
	[0.25]	[1.25]	[2.5]	[5.0]	[10]	
1.3×10^{17}	65±5	145±5	210±5	330±10	465±5	38.5
	[0.25]	[1.25]	[2.5]	[5.0]	[10]	
3.7×10^{17}	21±2	48±2	65±3	106±2	154±4	13.5
	[0.5]	[1.0]	[2.0]	[4.0]	[8]	
1.0×10^{18}	9±2	10±1	12±0.5	17.5±1	24±2	5.0
	[0.25]	[1.25]	[2.5]	[5.0]	[10]	
2.2×10^{18}	4±0.5	4.8±0.5	5.5±0.5	7.2±0.2	8.8±0.2	2.3
	[0.25]	[0.5]	[1.25]	[2.5]	[10]	
2.4×10^{18}	2.48±0.1	2.52±0.1	2.75±0.5	3.1±0.1	3.2±0.1	2.1
	[0.25]	[0.5]	[1.25]	[2.5]	[10]	
3.8×10^{18}	1.7±0.2	1.75±0.25	1.9±0.1	2.4±0.2	3.4±0.2	1.3

data of Nelson,[17] these results are remarkably smooth, and each characteristic is distinctly nonlinear with a characteristic shape similar to that expected for photon recycling (as will be demonstrated in Sec. V). This curvature makes

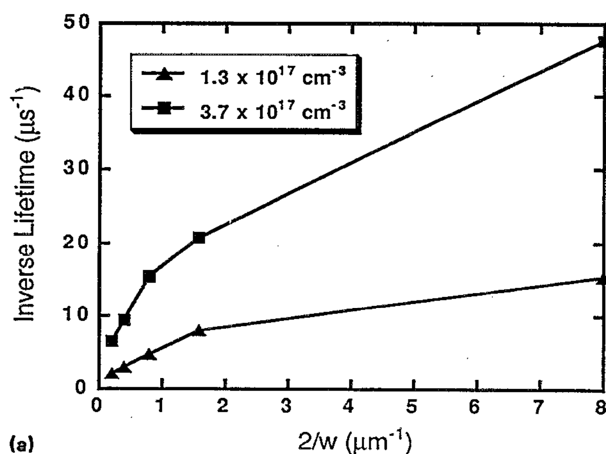

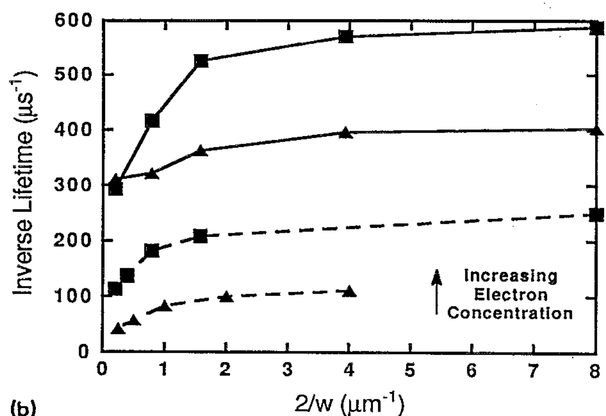

FIG. 4. The inverse decay rate vs $2/w$ for the DH samples with $n_0 = 1.3$ and 3.7×10^{17} cm^{-3} [part (a)], and the inverse decay rate vs $2/w$ for the DH samples with $n_0 \geqslant 1.0\times10^{18}$ cm^{-3} [part (b)]. The curvature observed is evidence for photon recycling.

TABLE III. Estimates for the interface recombination velocity for each electron concentration and the "surface lifetime," defined as $w/2S$, computed for the thinnest DH for each electron concentration.

n_0 (cm^{-3})	S (cm/s)	τ_S (ns)
1.3×10^{17}	115	109
3.7×10^{17}	417	30
1.0×10^{18}	454	55
2.2×10^{18}	648	19
2.4×10^{18}	157	80
3.8×10^{18}	412	30

determination of a unique S impossible, so we estimate S from the slope of the characteristic between the two thinnest DHs since those DHs are the most sensitive to interface recombination and the least sensitive to photon recycling. From Eq. (1) with the assumption that τ_{bulk} is either negligible or independent of w, we find

$$S \leqslant \frac{1}{2}\frac{1/\tau_{DH1}-1/\tau_{DH2}}{1/w_1-1/w_2}, \tag{4}$$

where the subscripts one and two refer to the thinnest DH and the second most thin DH, respectively. This procedure overestimates S because it ignores the thickness dependence of τ_{bulk}. The resulting upper limits for S at each electron density are listed in Table III. Also shown are the corresponding "surface lifetimes," defined as $\tau_S = w/2S$, computed for the thinnest DH at each electron concentration. These values of τ_S are quite long so we conclude that interface recombination is at most a small component of the decay rate for all DHs (with the possible exception of the thinnest films with $n_0 \leqslant 3.7\times10^{17}$ cm^{-3}). For the most part, therefore, the DHs may be regarded as "surface-free" since the observed decay constants are controlled by bulk recombination processes.

Because plots of $1/\tau_{DH}$ vs $2/w$ tell us nothing about τ_{bulk}, we plot τ_{DH} vs w for further insight. In these "surface free" DHs we can neglect the $2S/w$ term in Eqs. (1) and (2) and write

$$\tau_{DH}=\tau_{bulk}=\frac{\phi_r\tau_r\tau_{nr}}{\phi_r\tau_r+\tau_{nr}}, \tag{5}$$

where τ_{nr} is a combination of the SRH and Auger lifetimes. We expect ϕ_r to increase sevenfold or more as w increases from 0.25 to 10 μm.[8] If $\tau_{nr} \gg \tau_r$, then $\tau_{DH} \simeq \phi_r\tau_r$, and the change in τ_{DH} should be comparable to the expected change in ϕ_r. If τ_{nr} and τ_r are comparable, τ_{DH} will change less as w increases because τ_{DH} will approach τ_{nr} for large w. Figure 5 plots the normalized decay constants versus w for five of the electron densities. (DHs with $n_0 = 10^{18}$ cm^{-3} were left out since the thickest DH is 8 μm rather than 10 μm as with other electron concentrations.) The decay constants were normalized by dividing each τ_{DH} of a specific electron density by the value of τ_{DH} for the thickest sample at the same electron density. For $n_0 \leqslant 3.7\times10^{17}$ cm^{-3}, τ_{DH} varies most significantly (nearly sevenfold) with w, which suggests that these films are controlled by radiative recombination and photon recycling ($\tau_{nr} \gg \tau_r$). As

RIGHTSLINK

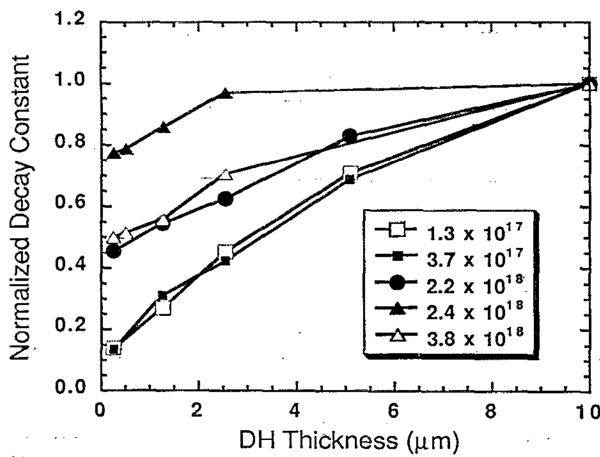

FIG. 5. Normalized decay constants vs DH thickness, w, for each of the six different electron densities. In each case, τ_{DH} is normalized to the value at $w=10$ μm. The films with $n_0 = 2.4 \times 10^{18}$ cm^{-3}, which were grown more slowly, show the least variation with DH thickness.

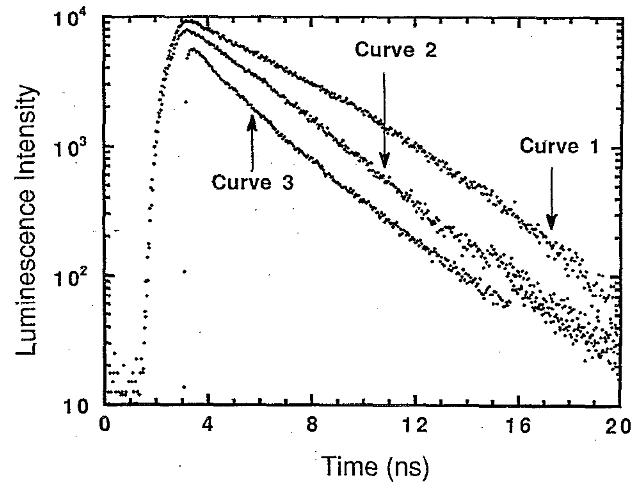

FIG. 7. Measured PL decays for the $n_0 = 3.8 \times 10^{18}$ cm^{-3}, 10-μm-thick DH at three laser intensities.

the electron concentration increases, the variation in τ_{DH} with DH thickness decreases. The τ_{DH} of the films grown at a reduced rate ($n_0 = 2.4 \times 10^{18}$ cm^{-3}) vary the least with DH thickness, indicating that nonradiative recombination dominates for the thickest DHs with $n_0 = 2.4 \times 10^{18}$ cm^{-3}. It is now of interest to determine which nonradiative mechanism is dominant in these DHs.

We have observed intensity dependence in the PL decays, and we now use this to show that the dominant nonradiative mechanism is SRH recombination. Figure 6 shows PL decays under various levels of laser excitation for the 10 μm DH with $n_0 = 1.3 \times 10^{17}$ cm^{-3}. At the highest intensity (curve 1), the photoluminescence decay shows a nonexponential characteristic with the initial decay being most rapid. This behavior is typical of bimolecular radiative recombination when the majority carrier concentration is perturbed. After the initial, fast transient, the PL decay is exponential, and τ_{DH} is readily extracted by a least-squares fit. For each of the lower intensity decays (curves 2–3), the characteristic is exponential with the same time constant, and those time constants are similar to that deduced from the high-intensity curve in the region following the rapid, initial decay.

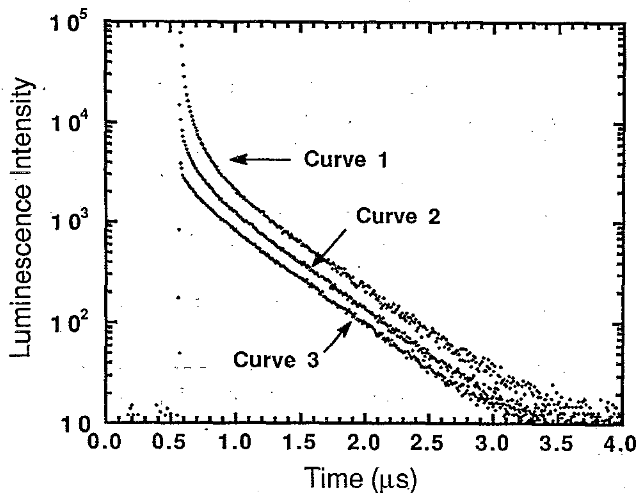

FIG. 6. Measured PL decays for the $n_0 = 1.3 \times 10^{17}$ cm^{-3}, 10-μm-thick DH at three laser intensities.

For DHs with higher electron concentrations, the intensity-dependent decays are more complex. Results for the 10 μm DH with $n_0 = 3.8 \times 10^{18}$ cm^{-3} are displayed in Fig. 7 for three different laser intensities. (We chose to perform these detailed studies on the films with $n_0 = 3.8 \times 10^{18}$ cm^{-3} rather than on those with $n_0 = 2.4 \times 10^{18}$ cm^{-3} because we felt that the former were more representative of the majority of the DHs.) At low laser excitation we see an exponential decay (curve 3) characterized by a single decay constant. As the excitation intensity is increased (curve 2), the PL decay becomes nonexponential with an initial decay rate that is slower than that observed under the lowest injection level. Under the highest laser excitation (curve 1), the initial decay rate is slower still. We find that the decay rate of curve 3 is similar to the decay rates at the end of curves 1–2. The arrows in Fig. 7 point to these regions of similar decay constants. The fact that the initial, rapid decay characteristic of bimolecular, radiative recombination is not observed shows that low-level injection conditions are maintained. We attribute the intensity dependence of the PL decays shown in curve 1 of Fig. 7 to variations in the SRH lifetime due to saturation of the deep levels.[29]

Under low injection conditions, and if $\tau_n \gg \tau_p$, the SRH recombination equation simplifies to

$$R=\frac{\Delta p}{(\Delta p/n_0)\tau_n+\tau_p}, \tag{6}$$

where Δp is the excess carrier concentration. If Δp is very small, $\tau_{SRH}=\tau_p$. However, if $\Delta p \tau_n \simeq n_0 \tau_p$, the deep levels become emptied and the effective SRH lifetime becomes

RIGHTSLINK

longer than τ_p. The intensity dependence of τ_{DH} is most prominent in the films with $n_0 = 2.4\times10^{18}$ cm^{-3}, which were grown at a slower growth rate than the other DHs. This correlates with the fact that these films exhibit the smallest thickness dependence and shows that the nonradiative recombination is dominated by SRH mechanisms.

The selenium concentration was measured for each electron concentration by secondary ion mass spectrometry (SIMS) in a Cameca IMS-3f using cesium as the ionizing source. It was found that the selenium concentration was approximately equal to the electron concentration for all films except those grown at 4 μm per hour (n_0=2.4 $\times10^{18}$ cm^{-3}), for which the actual selenium concentration was N_{Se}=4.1$\times10^{18}$ cm^{-3}. This extra selenium or perhaps additional background impurities incorporated due to the slower growth rate could be the cause of the shorter SRH lifetime. Remember, however, that even though SRH recombination is important, τ_{DH} for *each* film is greater than the estimated radiative lifetime (see Table II).

With the measurements reported here, we are unable to determine the contribution from Auger recombination. Nonetheless, we can set an upper limit on C_n, the Auger coefficient, if we attribute all the recombination in a DH to Auger mechanisms. We find that under high intensity excitation, the decay constant of the 10-μm-thick DH with $n_0 = 3.8\times10^{18}$ cm^{-3} yields an upper limit for C_n of 1.6 $\times10^{-29}$ cm^6/s, which is an order of magnitude smaller than $C_n = 1.5\times10^{-28}$ cm^6/s deduced by Puhlmann *et al.* Haug computed the C_n theoretically to be 0.47$\times10^{-29}$ cm^6/s in *n*-type GaAs.[11] Since SRH recombination is significant in our DHs at higher electron concentrations, the actual value of C_n in our material must be significantly smaller, so Haug's computation is not inconsistent with our results.

V. FURTHER EVIDENCE FOR PHOTON RECYCLING

The unusually long lifetimes observed and the curvature seen in plots of $1/\tau_{DH}$ vs $2/w$ suggest the presence of photon recycling. To show this more convincingly, Fig. 8 compares a theoretical calculation of $1/\tau_{DH}$ vs $2/w$ with the measured results for $n_0 = 3.7\times10^{17}$ cm^{-3}. We evaluate τ_{DH} from Eq. (1) assuming that $\tau_{bulk}=\phi_r\tau_r$ and compare the results to the measured data. Values for ϕ_r are taken from the literature.[8] Figure 8 shows that the measured characteristic is well-described by photon recycling theory if $S\simeq125$ cm/s. Figure 8 also shows that higher interface recombination velocities produce more linear characteristics. The smooth, nonlinear $1/\tau_{DH}$ characteristics observed indicate that the interface quality is excellent in these DHs.

In addition to increasing the observed lifetime, self-absorption should also cause a shift in the peak energy of steady-state photoluminescence (PL), due to the energy dependence of the absorption depth of spontaneous emission.[30] The peak of the observed steady-state PL for thicker DHs should be shifted in the direction of the red relative to that of the thinner films because the high-energy photons are more strongly absorbed in the thicker DHs before they can be emitted and detected. Figure 9 displays the steady-state PL spectra for DH films with $n_0 = 1.3\times10^{17}$ cm^{-3}. It is clear that the peak of the observed emission for the thicker films is shifted to the red relative to the peak of the observed emission of the thinner films. This red shift is evidence of self-absorption. We find that the amount of the red shift decreases with increasing electron concentration, indicating that *n*-GaAs becomes more transparent to its own emission at higher electron concentrations.

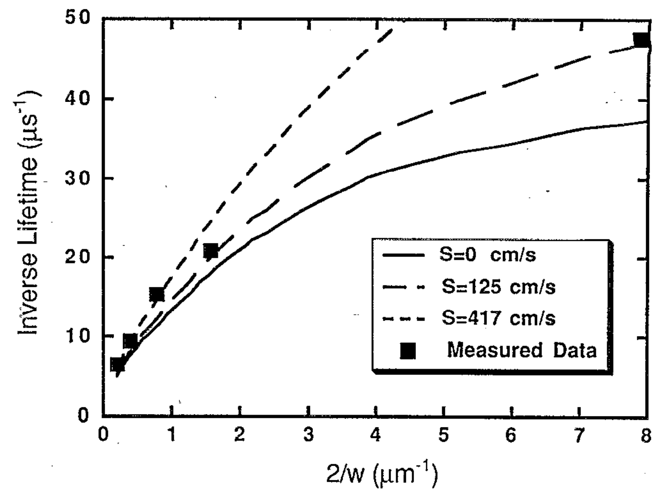

FIG. 8. Inverse decay constant vs $2/w$ computed theoretically assuming that bulk recombination is dominated by radiative recombination and photon recycling, and with interface recombination as a parameter. This figure shows that curvature in plots of $1/\tau_{DH}$ vs $2/w$ can be explained by photon recycling.

VI. CONCLUSIONS

In this article we have described a comprehensive study of minority carrier recombination in *n*-type GaAs.

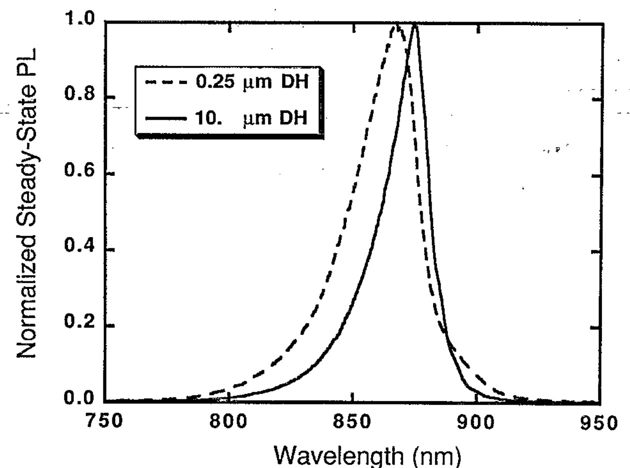

FIG. 9. Steady-state, room-temperature PL spectra for the AlGaAs/GaAs/AlGaAs double heterostructures for two GaAs layer thicknesses. For this particular sample, the GaAs layers have $n_0 = 1.3\times10^{17}$ cm^{-3}.

RIGHTSLINK

We find that the lifetime versus electron density characteristics can be described in terms of radiative and SRH recombination. For $n_0 < 10^{18}$ cm^{-3}, the lifetime appears to be dominated by radiative recombination and photon recycling. For $n_0 > 10^{18}$ cm^{-3}, SRH recombination is also observed, but radiative recombination is still important as evidenced by the curvature in plots of $1/\tau_{DH}$ vs $2/w$. Even for the most heavily doped films, we find no evidence of Auger recombination.

When compared to previous studies of LPE-grown films, our results for high-quality MOCVD films show significantly higher minority carrier lifetimes, especially at low electron densities. The reduced nonradiative recombination, attributed to lower defect densities, allows us to better investigate intrinsic recombination processes. Nevertheless, further work is needed before we are able to deduce the B coefficient or the Auger coefficient versus electron density. To estimate B, we need to compute the recycling cofactor, ϕ_r, which requires data for the concentration-dependent absorption coefficient, α. The reliability of available α data is uncertain since it may have been influenced by precipitates,[31] so new measurements of the concentration-dependent α are required. Studies of PL decay in thin-film DHs (with the absorbing substrate removed) may be useful because photon recycling should be enhanced. (Previous workers[32,33] have observed a tenfold or greater enhancement of PL intensity after removing the substrate.) Steady-state luminescence efficiency measurements as a function of incident intensity may produce a better assessment of the Auger recombination coefficient. The work described in this article is only the first step in gaining a full quantitative understanding of recombination in n-type GaAs, but it has established the importance of radiative recombination and photon recycling in MOCVD, n-type GaAs doped at the levels of interest for device applications.

ACKNOWLEDGMENTS

The authors would like to thank R. Alferos for his assistance in growing the double heterostructures at the Varian Research Center, and S. Asher for doing the SIMS measurements and D. Dunleavy for measuring steady-state PL at the National Renewable Energy Laboratory. This work was supported by the National Renewable Energy Laboratory and by Varian Associates.

[1] G. W. 't Hooft, C. Van Opdorp, H. Veenvliet, and A. T. Vink, J. Cryst. Growth **55**, 173 (1981).
[2] R. K. Ahrenkiel, *Minority Carrier Lifetime in Compound Semiconductors*, Current Topics in Photovoltaics (Academic, New York, 1988), Chap. 1.
[3] C. J. Hwang, J. Appl. Phys. **40**, 3731 (1969).
[4] C. J. Hwang, J. Appl. Phys. **42**, 4408 (1971).
[5] C. J. Hwang, Phys. Rev. B **6**, 1355 (1972).
[6] H. C. Casey, Jr., B. I. Miller, and E. Pinkas, J. Appl. Phys. **44**, 1281 (1973).
[7] N. Puhlmann, G. Oelgart, V. Gottschalch, and R. Nemitz, Semicond. Sci. Technol. **6**, 181 (1991).
[8] R. K. Ahrenkiel, D. J. Dunlavy, B. Keyes, S. M. Vernon, T. M. Dixon, S. P. Tobin, K. L. Miller, and R. E. Hayes, Appl. Phys. Lett. **55**, 1088 (1989).
[9] D. Z. Garbuzov, *Semiconductor Optoelectronics*, edited by M. A. Herman (Wiley, New York, 1980), pp. 305–343.
[10] M. Takeshima, J. Appl. Phys. **58**, 3846 (1985).
[11] A. Haug, J. Phys. C **16**, 4159 (1983).
[12] L. R. Weisberg, J. Appl. Phys. **39**, 6096 (1968).
[13] L. Jastrzebski, J. Lagowski, H. C. Gatos, and W. Walukiewicz, *Gallium Arsenide and Related Compounds* (Institute of Physics, London, 1979), p. 437.
[14] D. J. Wolford, G. D. Gilliland, T. F. Kuech, L. M. Smith, J. Martinsen, J. A. Bradley, C. F. Tsang, R. Venkatasubramanian, S. K. Ghandi, and H. P. Hjalmarson, J. Vac. Sci. Technol. B **9**, 2369 (1991).
[15] J. M. Olson, R. K. Ahrenkiel, D. J. Dunlavy, B. Keyes, and A. E. Kibbler, Appl. Phys. Lett. **55**, 1208 (1989).
[16] R. K. Ahrenkiel, Solid State Electron. (Special Edition: Semiconductor Measurement Techniques) (in press).
[17] R. J. Nelson, J. Vac. Sci. Technol. **15**, 1475 (1978).
[18] A. Many, Y. Goldstein, and N. B. Grover, *Semiconductor Surfaces* (Wiley, New York, 1965).
[19] R. K. Ahrenkiel, D. J. Dunlavy, B. M. Keyes, S. M. Vernon, S. P. Tobin, and T. M. Dixon, *Conf. Rec., 21st IEEE Photovoltaic Specialists Conf.* (IEEE, New York, 1990).
[20] P. Asbeck, J. Appl. Phys. **48**, 820 (1977).
[21] R. J. Nelson and R. G. Sobers, J. Appl. Phys. **49**, 6103 (1978).
[22] O. von Roos, J. Appl. Phys. **54**, 1390 (1983).
[23] H. F. MacMillan, H. C. Hamaker, N. R. Kaminar, M. S. Kuryla, M. Ladle Ristow, D. D. Liu, G. F. Virshup, and J. M. Gee, *Conf. Rec., 20st IEEE Photovoltaic Specialists Conf.* (IEEE, New York, 1988), p. 462.
[24] E. Yablanovitch, T. Gmitter, J. P. Harbison, and R. Bhat, Appl. Phys. Lett. **51**, 2222 (1987).
[25] D. D. Sell and H. C. Casey, Jr., J. Appl. Phys. **45**, 800 (1974).
[26] R. Z. Bachrach, Rev. Sci. Instrum. **43**, 734 (1972).
[27] R. K. Ahrenkiel, D. J. Dunlavy, and T. Hanak, J. Appl. Phys. **64**, 1916 (1988).
[28] D. E. Aspnes, S. M. Kelso, R. A. Logan, and R. Bhat, J. Appl. Phys. **60**, 754 (1986).
[29] R. K. Ahrenkiel, B. M. Keyes, and D. J. Dunlavy, J. Appl. Phys. **70**, 225 (1991).
[30] R. K. Ahrenkiel, B. M. Keyes, G. B. Lush, M. R. Melloch, M. S. Lundstrom, and H. F. MacMillan, J. Vac. Sci. Technol. (in press).
[31] H. C. Casey, Jr. and F. Stern, J. Appl. Phys. **47**, 631 (1976).
[32] J. L. Bradshaw, W. J. Choyke, R. P. Devaty, and R. L. Messham, J. Appl. Phys. **67**, 1483 (1990).
[33] D. Z. Garbuzov, *Semiconductor Physics*, edited by M. M. Tuchkevich and V. Y. Frenkel (Consultants Bureau, New York, 1986), pp. 53–86.

RIGHTSLINK